10C.4 EXAMINING EXTRATROPICAL TRANSITION OF ERNESTO WIND FIELDS AND DEVELOPING STORM SURGE

John Billet[1]*, Harry V. Wang[2], Leonidas Linardakis[2], and Tao Shen[2]

[1]NOAA/NWS, Wakefield, VA
[2]Virginia Institute of Marine Science, Gloucester Point, VA

1. INTRODUCTION

Ernesto caused significant damage across the southern Chesapeake Bay after it had been downgraded to a tropical depression. As Ernesto moved into Virginia, wind gusts exceeded hurricane force at some locations along the Chesapeake Bay. These strong winds combined with a prolonged east flow produced significant storm surge flooding for some Chesapeake Bay communities.

Ernesto made its final landfall in southern North Carolina at 0300 UTC September 1, 2006, and by 1800 UTC it had reached the North Carolina/Virginia border where it was rapidly undergoing extratropical transition. It was an extratropical cyclone as it crossed Virginia and Maryland with sustained winds around 40 kts, and then weakening quickly by the time it reached Pennsylvania. Hart and Evans (2001) showed that the mid-Atlantic is an area to watch for extratropical transition, especially during August to September. The distance between, when the tropical cyclone makes landfall and weakens and where it interacts with baroclinic processes must be close enough that the tropical cyclone does not entirely decay before the baroclinic processes can begin to intensify the circulation Hart and Evans (2001). This closeness and the factors that helped this transition will be explored from an operational meteorology perspective. This paper will provide forecasters with tools that can help in forecasting the increasing wind and wind field size which frequently occurs after the extratropical transition.

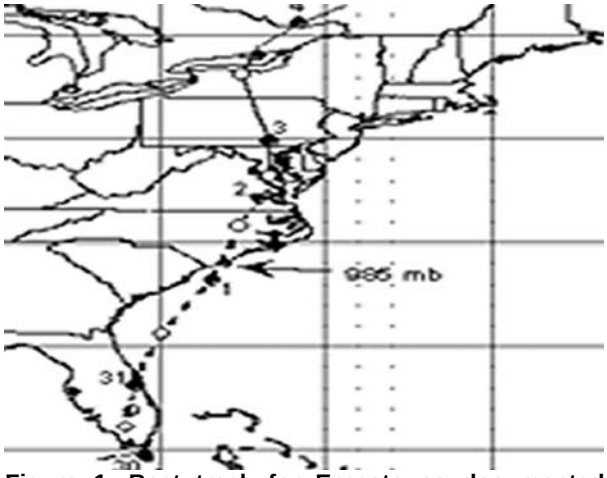

Figure 1. Best track for Ernesto as documented from the National Hurricane Center.

As part of this study, several variations of the Weather Research and Forecasting Environmental Modeling System (WRF EMS; Rozumalski, 2006) used at most National Weather Service forecast offices, were used to examine the transition and the increased wind fields. A large high pressure center to the north of Ernesto produced a prolonged period of east winds. As Ernesto transitioned into an extratropical cyclone, these easterly winds increased and expanded in area. This led to significant storm surge flooding. An improved method of predicting this storm surge is explored.

2. EXAMINATION OF ERNESTO'S EXTRATROPICAL TRANSITION

There are several parameters to examine when watching for extratropical transition. Expansion of the circulation at upper levels, a developing asymmetry to the storm, and stronger temperature gradients in the storm were shown by Evans and Hart (2008) to occur during extratropical transition. Klein (2001), in looking at the extratropical transition of typhoons, showed the advantages of using cross sections of theta-e, winds, potential vorticity (PV) and vertical motion to better observe the transition to extratropical. In this study use of numerical models such as North American Mesoscale Model (NAM) Rogers (1995), Global Forecast Systems Model (GFS) Environmental Modeling Center (2003) and Rapid Update Cycle model (RUC) Benjamin (2002) will be used to examine the potential for the system to become extratropical.

Examining a cross section of Ernesto (Fig. 2) shows the vertical stacking of the potential vorticity near landfall. It also depicts the symmetry around the center for the vertical motion. These factors are consistent with a tropical system beginning to weaken over land. In examining theta-e at the same time, the warm core is still vertically stacked (not shown).

* Corresponding author address: John Billet, National Weather Service 10009 General Mahone Hwy Wakefield, VA 23888; email: John.Billet@noaa.gov

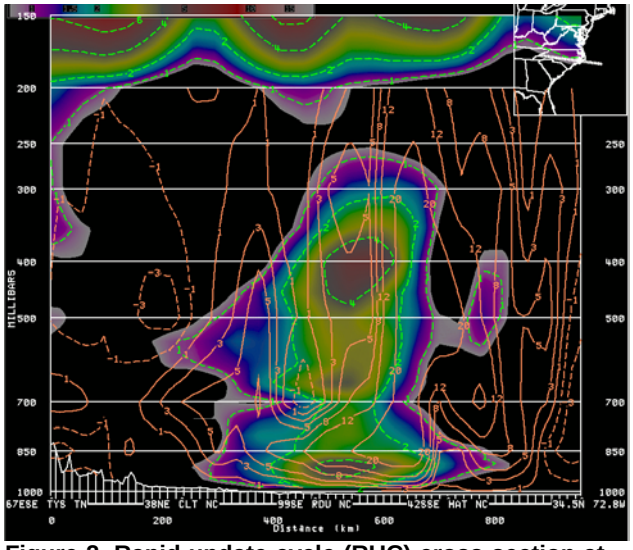

Figure 2. Rapid update cycle (RUC) cross section at 1000 UTC on 01 Sep 2006 of potential vorticity (shaded, PVU) and vertical velocity (contoured, m s^{-1}). Positive vertical motion is indicated with solid brown isotachs.

In determining if a transition might occur, one of the ingredients is an interaction with a mid-latitude upper level system. This is the case with Ernesto as a strong jet is located across New England (Fig. 3). Strongest winds in this jet are near 120 kts. There is also a strong front located just to the north of Ernesto, near the Virginia/North Carolina border. The interactions between Ernesto and the jet streak and front will aid in the extratropical transition and allow the storm winds to increase.

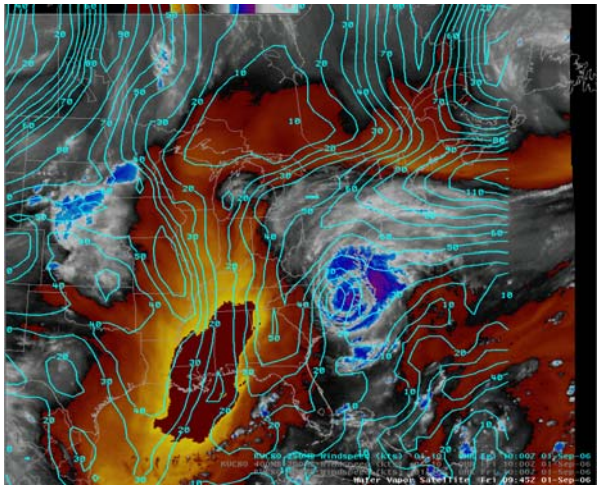

Figure 3. Water vapor satellite image valid on 1000 UTC 01 Sep 2006 . The solid lines are isotachs (kts.) at 250 hPa.

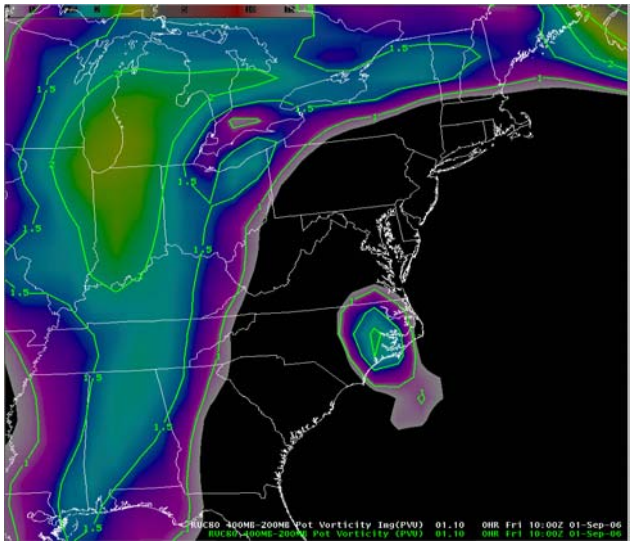

Figure 4. RUC 00 hr potential vorticity (PVU) at 500 hPa valid at 1000 UTC 01 Sep 2006

Fig. 4 shows the potential vorticity from the upper system to the west approaching Ernesto just as it is making landfall. The potential vorticity coming in from the west will provide the energy to increase and re-strengthen Ernesto resulting in an increase in the wind field.

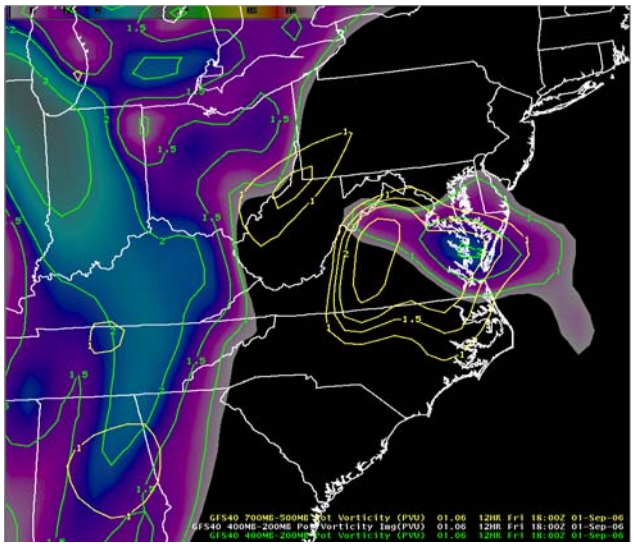

Figure 5. 12-hour forecast potential vorticity (PVU) valid at 18 UTC 01 Sep 2006. Shading and green contours are at 500 hPa, and yellow contours are at 700 hPa.

Fig. 5 in plan view shows the slope of PV which has developed within 12 hours of landfall. This forecast from the GFS was very close to the observed data. The potential vorticity to the west is wrapping into the system and helping to increase and sustain the potential vorticity in the remains of Ernesto.

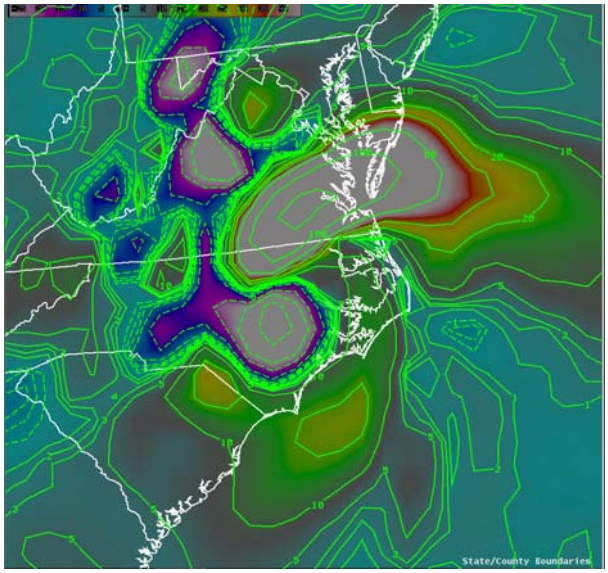

Figure 6.RUC analysis Petterson frontogenesis (units of K m^{-1} x10^{10} s^{-1}) in the layer 1000 hPa to 850 hPa valid at 1200 UTC 01 Sep 2006.

The interaction with the front to the north also changes the character of the storm. The initial maximum of the frontogenesis was only a third of what develops just 6 hours later shown in Fig 6. The GFS also shows this strong increase in Petterson frontogenesis (not shown). This helped to fuel the heavy convective rains which developed across southeastern Virginia at this time. This heavy convective rainfall is developing the potential vorticity to increase Ernesto's circulation.

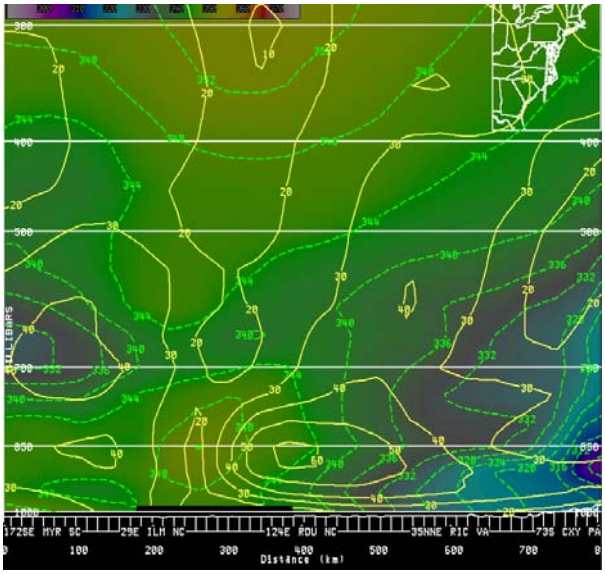

Figure 7. RUC analysis valid at 1000 UTC 01 Sep 2006 of theta-e (K, green dashed and color fill), and winds (kts, solid yellow).

Fig. 7 shows the vertical structure of theta-e near landfall. However, there is already an asymmetry to the wind field as shown with the higher winds to the east. A 12-hour forecast from the RUC almost completely eliminates the warm core within the center of the storm and now has the highest theta-e air to the east and develops even more asymmetry in the wind field. This change is shown in Fig. 8.

By running a high resolution 4 km WRF-EMS, more details can be obtained during the extratropical transition. This will provide additional information to the forecaster to determine how the transition will occur and if strengthening can be expected of the storm post landfall.

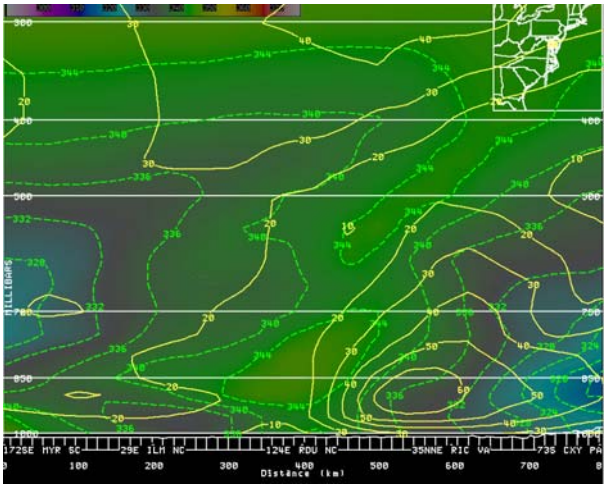

Figure 8. Same as in Figure 8 except for the 12-hour projection valid 22 UTC 01 Sep 2006.

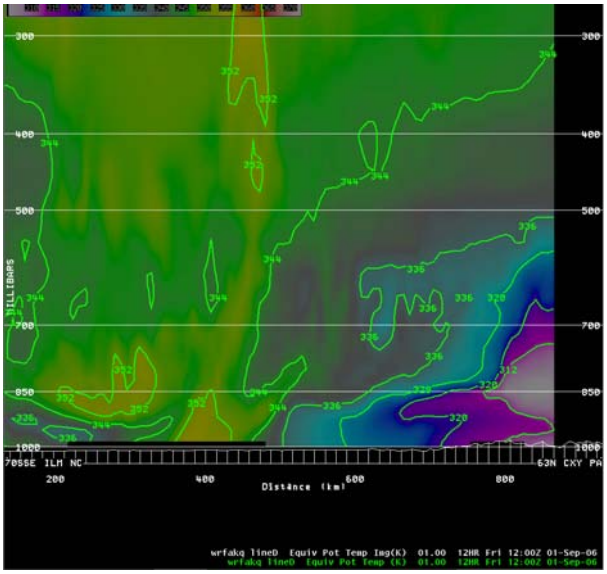

Figure 9. North south cross section like Figure 9 of Local WRF-EMS model 12 hour forecast valid at 1200 UTC on 01 Sep 2006 of theta-e (K).

Fig. 9 shows a north-south cross section near landfall through the storm. The warm core is nearly vertical, with the driest air to the north behind the front. The model shows a dramatic change 12 hours later, with a significantly sloped surface and a more baroclinic look to the storm (Fig. 10.). This shows Ernesto changing to

extratropical as temperature gradients and thermal wind forcing becomes the dominant forcing on the circulation.

The wrapping of the higher theta-e air to the north of the circulation as shown in Fig 11 with the addition of drier air near the cyclone center, advecting into the system from the southwest has been documented in other studies as the system has made the transition to extratropical (Klein 2001)

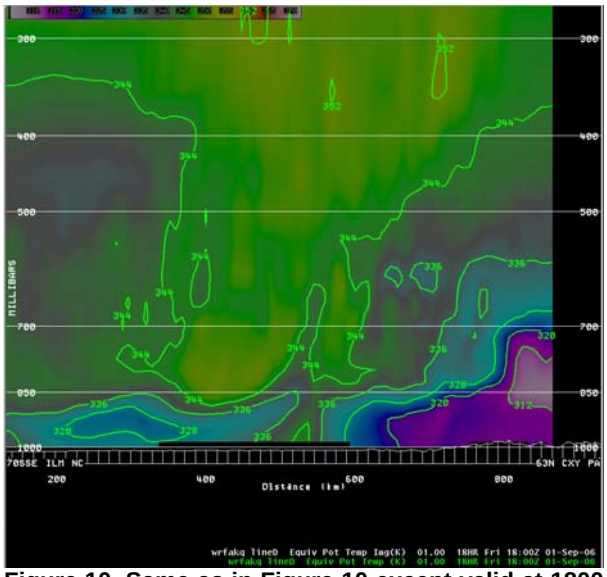

Figure 10. Same as in Figure 10 except valid at 1800 UTC 01 Sep 2006.

The WRF model shows these details well, and examination of the model at the higher resolution provides new details to the forecaster.

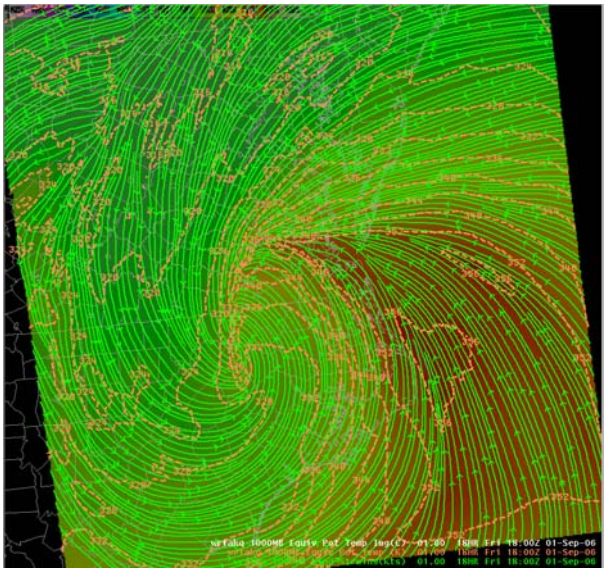

Figure 11. WRF-EMS 18 hour forecast valid at 18 UTC 01 Sep 2006 with streamline and theta-e image. Image is red for the higher values and green for lower values of theta-e.

While all models show this transition to some extent, the local high resolution WRF-EMS model does the best at expanding this wind field, particularly at higher wind speeds.

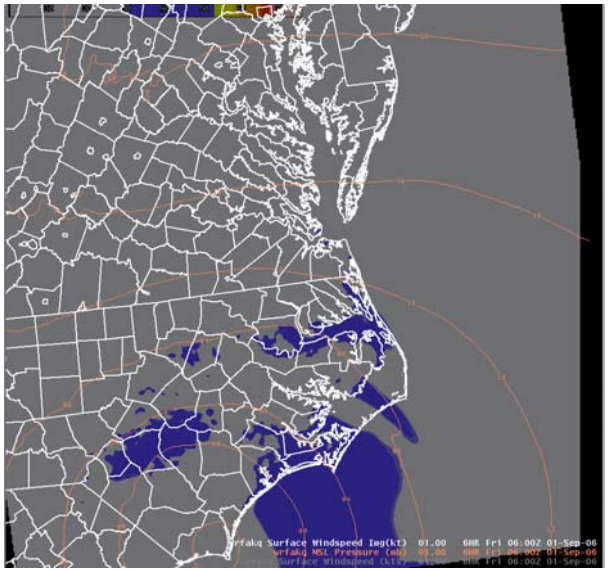

Figure 12. Local WRF-EMS 6 hour forecast of mean sea level pressure (MSLP, hPa) and wind speed (kts) valid at 0600 UTC on 01 Sep 2006. Wind speeds greater than 30 kts are shaded in blue.

A look at the WRF-EMS winds (Fig. 12) show the smaller area covered by winds greater than 30 kts at landfall. While Fig. 13 shows the marked increase in area that occurs just 6 hours later. While this is a 12 hour forecast, the RUC analysis shows this verified well.

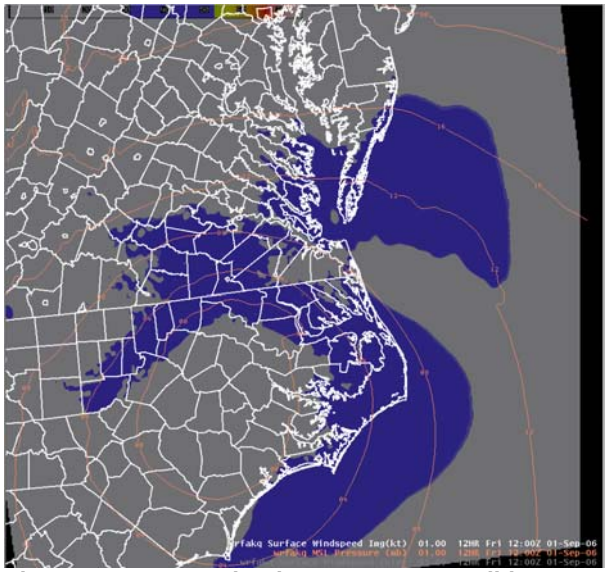

Figure 13. Same as in Figure 12 except valid at 1200 UTC 01 Sep 2006.

3. WRF EMS COMPARISON

The WRF EMS has numerous options for configuration at the local forecast office. In this paper just some of the options which take the least computer resources will be examined. This will help forecasters judge if it is worthwhile to reconfigure a model when the threat of a storm becoming extratropical is approaching the area.

3.1 Model Experimental Design

The simplest change to the WRF-EMS is to change the boundary conditions. In this case we used the GFS 40 km for one run (WRF GFS) and the NAM 12 km for a second run (WRF NAM). A third run used the GFS boundary condition but with an additional 8 vertical levels of which 6 were located below 900 hPa and the two other levels near 850 hPa to help improve the model's vertical resolution (WRF LVLS). All other runs had 31 vertical levels while this run had 39. A final run was made with the core of the model changed to the Advanced Research WRF (ARW) version (WRF ARW). All the other runs used the NMM core. All models were not nested but had 4 km grid spacing with either the NAM 12 or GFS 40 as the boundary condition. The radiation and boundary schemes were the same as run in the NAM 12 model and convection was explicitly resolved. All model runs were initialized on 1200 UTC on August 31, 2006 and run for 30 hours.

3.2 *Model Comparisons*

The NAM boundary conditions for the WRF NAM run had Ernesto tracking significantly farther south and west compared to the observed track. Meanwhile the GFS was close to the observed track. For example the WRF NAM forecast based on the NAM boundary conditions located the center of Ernesto over 300 km southwest of the observed location for the 30 hour forecast, while at the same time the WRF GFS with the GFS boundary condition was only 100 km to the west. This would suggest that the WRF GFS produced the best wind field for Ernesto. At Yorktown, VA (Fig. 14) and Chesapeake Bay Bridge Tunnel, VA (Fig. 15) the wind speed from the WRF GFS is the closest to the observed wind speeds. The trend of the wind speed also resembles the observational data better than the WRF NAM.

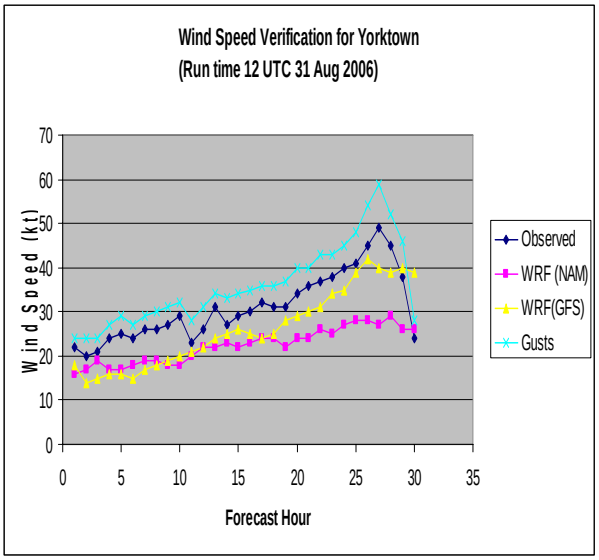

Figure 14. Yorktown, VA, observed and modeled winds and gusts (kts).

The WRF GFS follows the trend of increasing winds the best. It even picks up some of the decrease in speed at the very end of the model run. This trend can be useful in the forecast process to produce the correct pattern for the wind field. The WRF GFS runs had the best trend of the wind field at the majority of verification points used. The wind speed root mean square error for all points with the WRF NAM was near 8 kts. for the WRF GFS 6 kts. The WRF GFS was significantly better in the first 20 hours and then showed a high bias with generally poor performance during later periods.

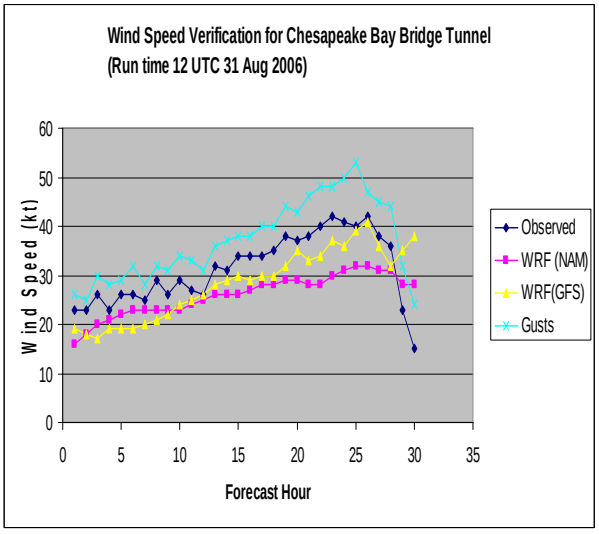

Figure 15. Chesapeake Bay Bridge Tunnel plotted observed winds and gusts with each model speed in kts.

The addition of extra vertical levels (WRF LVLS) in the models does not make an appreciable difference (Fig. 16). This model run also used the GFS as the boundary condition and the placement of Ernesto at 30 hours was

80 km southwest of the observed location. However, the mean sea level pressure was 988 hPa over 10 hPa

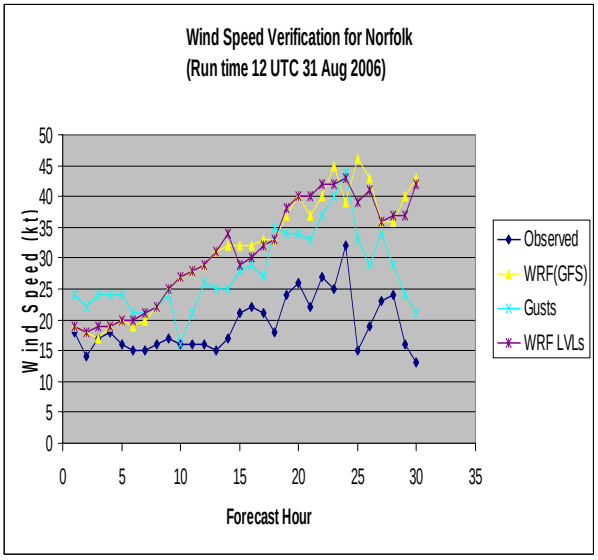

Figure 16. Plotted wind speed of the observations and gusts with the model speeds in kts.

to low. The pattern of winds which developed, while too strong, was similar to what was observed. The errors and patterns were extremely similar to the WRF GFS. The plot in Figure 16 shows the similarity for Norfolk, VA. In this case, the WRF LVLS verified slightly better then the WRF GFS.

The final model run was conducted using the ARW model core, and with the GFS boundary conditions (WRF ARW). The WRF ARW model performed similar to the WRF GFS.

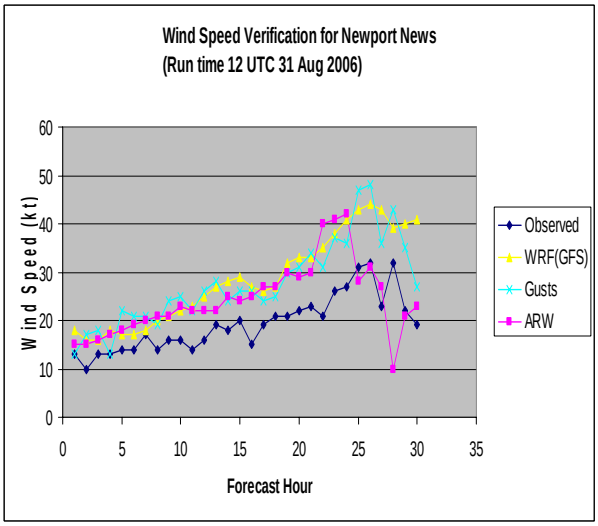

Figure 17. Plotted wind speed of the observations and gusts with model speeds in kts.

At Newport News, VA the WRF ARW version of the model performed better than the WRF NAM version (Fig 17). The one area the WRF ARW did better is to show the significant decrease in the last few hours of the winds. This was shown at every station examined. However, this model needs to be smoothed and run with a much smaller time step or waves appear through the latter half of the solution. With the type of computer clusters at local forecast offices, these simulations suggest that the simplest is the best. The boundary conditions play a major role in the overall solution of the model, but because of the high wind speed bias in all the models shown, the WRF NAM when looking at all locations had the lowest root mean square error. This is due to the generally lower wind speeds due to the center of Ernesto being so much farther to the southwest. With a known bias forecasters can make adjustments and then the model of choice becomes the WRF GFS as this produces the best patterns that resemble observations.

4. MODELING STORM SURGE DURING ERNESTO

Although Ernesto was downgraded to a tropical depression as it reached the Chesapeake Bay (Fig. 1), it still caused significant storm surge and flooding in the southern portion of the Bay. As shown in Figure 18, the storms' tide reached 1.2 m at the Chesapeake Bay Bridge Tunnel, 1.3 m at Sewells Point, 1.3 m Windmill Point, 1.4 m at Lewisetta and, further north, 1.1 m at Solomon's Island. The magnitude of the storm surge (storm tide less than astronomical tide) was comparable to the hurricane-induced storm surge in the Bay (Stamey et al. 2007). The cause of the relatively large storm surge was not Ernesto, rather it was the direct consequence of a persistent northeasterly wind with the speed exceeded 30 knots for 2-3 days offshore of the Chesapeake Bay mouth, as the results of the interaction between Ernesto and a high pressure centered north of New England with a ridge down the east coast.

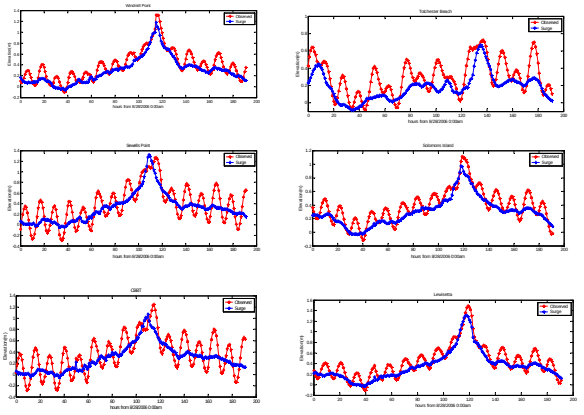

Figure 18. The observed water elevation (m) in the Chesapeake Bay during tropical storm Ernesto; storm tide (red) and storm surge (blue)

4.1 *Numerical model*

The numerical model ELCIRC (Eulerian Lagrangian Circulation) model originally developed by Zhang et al. (2004) was used for simulating this unusual storm surge event. The model uses an orthogonal, unstructured grid with mixed triangular and quadrilateral grids in the horizontal, and the z-coordinate in the vertical. It was modified extensively, including a modification of the inundation scheme and locally mass conserving scheme (Wang, C. F. et al., 2007). The model allows robust wetting-and-drying with semi-implicit scheme and can simulate storm surge using a high-resolution grid, while still maintaining a relatively large time step. This is due to the use of Eulerian Lagrangian scheme which does not have a CFL (Courant-Friedrichs-Levy) stability criteria and thus allow the choice of time step to be decoupled from the spatial resolution. The model has been successfully used for hurricane-induced storm surge studies (Wang et al., 2005; Shen, J. et al., 2006a; Shen J., et al. 2006b).

4.2 The set-up of a large grid domain

In the initial set-up for the Ernesto simulation, a limited model domain covering the entire Chesapeake Bay and a portion of the adjacent continental shelf (extending 150 km from the FRF facility, NC in the south to the Ocean City, MD in the north, and 60 km offshore from the Bay mouth in the east) was used. This domain was not adequate for simulating storm surge induced by Ernest because Ernesto was transformed to a much larger scale extra-tropical system; obviously, the limited domain was too small to cover the scale of the system. This created a difficulty in specifying a proper water elevation for the open boundary condition on the limited domain. Eventually, a decision was made to generate a large grid domain that encompasses a portion of the Western Atlantic Ocean from Nova Scotia to Florida with the high-resolution Chesapeake Bay located in the mid-latitude, as shown in Figure 19. With

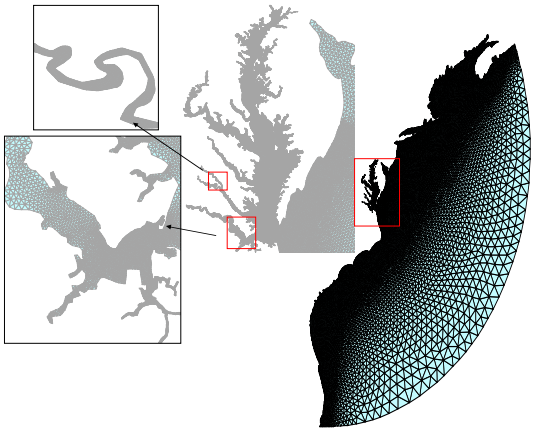

Figure 19. The large model grid domain that extends from Nova Scotia to Florida with the high-resolution Chesapeake Bay domain located in the mid-latitudes.

this domain, the outer open boundary is far into the Atlantic Ocean beyond the continental shelf. The ocean tidal harmonics - M2, N2, S2, K1, O1, K2, and Q1 – obtained from the ADCIRC model in SMS (www.ems-i.com) were then specified at each location of the open boundary. A Manning coefficient 0.015 was used for the bottom friction based on the tidal calibration inside the bay and along the coast. The surface wind stress drag coefficient used is from Garratt (1977):

$$C_d = (0.75 + A_{w1} |W|) \times 10^{-3}$$

if $C_d > 0.003$, $C_d = 0.003$

Where $A_{w1} = 0.067$; $|W|$ is the wind speed

5. THE RESULTS OF WIND FORCING FIELD AND THE STORM SURGE SIMULATION

For the Ernesto simulation, the storm surge simulation started August 28, 2006 and ended on September 6, with the peak of the storm surge occurred at September 1, 2006. When the storm surge model was set up and run, it was first spun-up for 7 days with astronomical tidal currents created by seven tidal constituents specified at the open boundary condition. After spun up, it was then coupled with the wind field interpolated from the results of the atmospheric model onto the unstructured grid using bi-linear interpolation scheme.

The surface wind (at 10 m height) and pressure field , provided by the National Weather Service, Wakefield Office was the product of a hybrid 4-km local WRF-EMS (for the Chesapeake Bay region) using NAM as the boundary condition and the global NCEP 12-km wind (for the vast ocean area). A continuous wind forcing

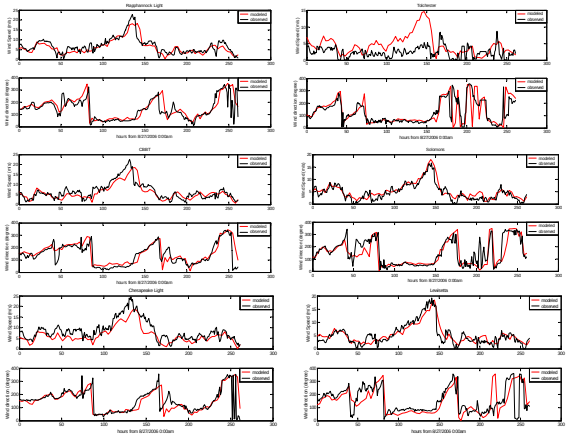

Figure 20. The comparison of modeled and observed wind field (its magnitude and direction) at 6 locations in the Chesapeake Bay.

and pressure field was generated by piecing together from the 12-hour portion of the 36-hour forecast consecutively from August 28 through September 6.

This continuous wind and pressure field was then used for driving the storm surge model.

The modeled wind fields compared with observations are shown in Figure 20. The comparisons showed that the wind magnitude and direction for most of the stations (about 17 meteorological stations) inside the Chesapeake Bay were very reasonable. There are exceptions, however, as near the middle portion of the Bay around Rappahannock River and in the Northern Bay. In the Rappahannock, the modeled wind was under-predicted by approximately 5 m/sec , whereas in the Upper Bay near Tolchester Beach, the modeled wind over-predicted by 5-10 m/sec. The sensitivity test showed that these deficiencies on wind field can result in 10-15 cm differences of water level in the storm surge simulation. These differences thus are not minor and have impacts on the quality of the local storm surge simulation. Given the storm surge was known to sensitive to the winds in the Bay (local wind), an objective scheme - the Barnes scheme based on the 2D technique of Koch et al. (1983) – was used to correct the deficiency between the observed and the modeled wind fields for above locations. The purpose was to reconstruct a well-represented wind field as the forcing function for the storm surge model.

Using this reconstructed wind field, the simulated storm surge water elevation results were quite satisfactory as compared with the available water level observation in the Bay. Figure 21 shows the storm tidal simulations at four stations: CBBT, Windmills Point, Solomon's Island and Tolchester Beach, representing Bay mouth, lower, middle, and upper Bay respectively. The correlation coefficient-squares are around 0.9 and absolute errors were approximately10 cm. With the same wind forcing, a similar simulation was conducted in a smaller, limited domain, and the results (not shown) significantly underestimated the primary storm surge response. This demonstrated that the storm surges are sensitive to the size of the model domain. An adequate domain size chosen should be larger or the same scale of the storm

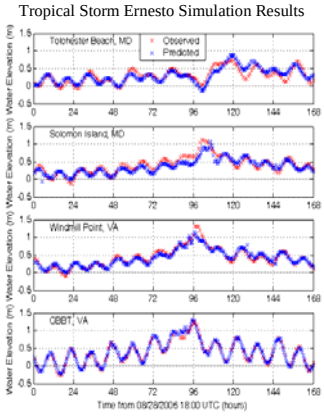

Figure 21. The tropical storm Ernesto simulation results versus observation; observation (red) and model results (blue).

system, if a tidal open boundary condition is to be applied. Overall, the result presented here demonstrated that the unstructured grid model on a large domain is capable of simulating the storm surge induced by an extra-tropical cyclone system such as Ernesto, if the domain size was properly chosen and boundary condition was adequately specified.

6. CONCLUSIONS

Determining whether a storm is going through extratropical transition can give the meteorologist information that is required to improve the forecast. Knowledge that the wind field will be expanding and that some re-intensification is possible will lead to improved watches and warnings to the public.

This study showed a practical application of looking at Ernesto as it was transitioning to an extratropical storm. One of the first aspects to look for is if there will be an interaction with a mid-latitude system. In this case it was an upper trough and a strong northern stream jet. As part of this process, a look at the upstream potential vorticity is also needed. Another tool is to take a cross section through the storm and see how the potential vorticity changes in time. As the potential vorticity becomes less vertically stacked and increases in the lower levels, this helps to maintain or even increase the wind field. Another cross section showing the wind field and theta-e can track the asymmetry developing in the wind as well as the cooling of the central core. Finally, looking at frontogenesis will show the storm becoming baroclinic and the developing frontal zone will aid the wind flow.

The local high resolution WRF model can provide the details necessary to develop 5 km grid scale forecasts as are done by the National Weather Service. This paper showed that in this case the simplest version of the model performed as well as a more sophisticated version. With the limited resources for computationally expensive model runs local offices, this provides confidence in making the quickest run of the model. Also understanding a bias in the model can lead to making proper adjustments to wind speeds to be closer to observations. Using the model trends, however, was shown at locations to significantly improve the forecast and this detail is not available in the national models where output is 3 hourly or longer, versus hourly in the local models.

In this effort, we have concluded that that the storm surge modeling due to northeaster-like system (such as Ernesto) can be simulated adequately. The lessons learned are: (1) The storm surge simulation is sensitive to the scale of the atmospheric system (2) A large grid domain is feasible for simulate northeaster-like events, given the grid domain is properly constructed and model executed, and (3) The storm surge are sensitive to the local wind inside the Bay as well. The assimilation of observation wind field in the Mid-Bay and the Upper Bay

stations for the Ernesto event improve the storm surge modeling results.

Disclaimer

Mention of a commercial company or product does not constitute an endorsement by the National Weather Service. Use of information from this publication concerning proprietary products or tests of such products for publicity or advertising purposes is not authorized.

REFERENCES**

Benjamin, S. G., and Coauthors, 2002: RUC20—The 20-km version of the Rapid Update Cycle. NOAA Tech. Memo. OAR FSL twenty eight. Forecast Systems Laboratory, Boulder, CO, 9 pp.

Environmental Modeling Center, 2003: The GFS Atmospheric Model. NOAA/NCEP/Environmental Modeling Center Office Note 442, 14 pp. [Available http://www.emc.ncep.noaa.gov/officenotes/FullTOC.html]

Evans, C and R.E. Hart, 2008: Analysis of the Wind Field Evolution Associated with the Extratropical Transition of Bonnie (1998). *Mon. Wea. Rev. Accepted for 2008.*

Garratt, J. R., 1977: Review of Drag Coefficients over Oceans and Continents. *Mon. Weather. Rev. Vol105, pp 915-929*

Hart R. E. and J. I. Evans, 2001: A Climatology of the Extratropical Transition of Atlantic Tropical Cyclones, *J. Climate,* **14**, 546-564.

Klein, P. M., P. A. Harr, and R. L. Elsberry, 2000: Extratropical transition of northwest Pacific tropical cyclones: an overview and conceptual model of the transformation stage. *Wea. Forecasting*, **15**, 373-395.

Koch, S. E., M. Desjardins and P. J. Kocin, 1983: An interactive Barnes objective map analysis scheme for use with satellite and conventional data. *J. Climate and Appl. Meteor.*, 22, 1487-1502.

Rogers, E., D.G. Deavan, and G. J. DiMego, 1995: The Regional Analysis System for the Operational "Early" Eta Model: Original 80-km Configuration and Recent Changes. *Wea. Forecasting*, **10,** 810–825

Rozumalski, R. A., 2006: SOO/STRC WRF EMS User's Guide. http://strc.comet.ucar.edu/wrf

Shen, J, H. V. Wang, M. Sisson, and W. Gong, 2006 a: Storm tide simulation in the Chesapeake Bay using an unstructured grid model. *Estuarine*, *Coastal and Shelf Science,* **68 (1-2),** 1-16.

Shen, J., W. Gong, and H.V. Wang, 2006b: Water level response to 1999 hurricane Floyd in the Chesapeake Bay. *Cont. Shelf Res*, **26**, 2484-2502.

Stamey, B. H., V. Wang and M. Koterba , 2007: Predicting the next storm surge flood". *Sea Technology,* **48**, 10-15.

Wang, C. F.. H. V. Wang and A. Kuo, 2007: A mass conservative transport scheme for application of ELCIRC model to water quality computation". (in review).

Wang, H. V, J. Cho, J. Shen, and Ya Ping Wang, 2005: "What has been learned about storm surge dynamics from Hurricane Isabel model simulations?" Hurricane Isabel *in Perspective Conference, Baltimore, MD., Proceedings, Chesapeake Bay Consortium,* 117-125.

Zhang, Y.-L., A.M. Baptista, and E. P. Myers, 2004: A cross-scale model for 3D baroclinic circulation in estuary-plume-shelf systems: I. Formulation and skill assessment. *Cont. Shelf Res.*, **24**, 2187-2214.